Conformational Studies of Cyclopropylmethyl Isothiocyanate from Temperature-Dependent FT-IR Spectra of Rare Gas Solutions and Ab Initio Calculations

Chao Zheng,[†,‡] Gamil A. Guirgis,[§] Wouter A. Herrebout,[||] Benjamin J. van der Veken,[||] Charles J. Wurrey,[†] and James R. Durig*[,†]

Department of Chemistry, University of Missouri−Kansas City, Kansas City, Missouri 64110, Department of Chemistry and Biochemistry, College of Charleston, Charleston, South Carolina 29424, and Department of Chemistry, University of Antwerp, Groenenborgerlaau 171, B2020 Antwerp, Belgium

Received: January 18, 2006; In Final Form: May 11, 2006

Variable temperature (−55 to −150 °C) studies of the infrared spectra (3200−100 cm^{-1}) of cyclopropylmethyl isothiocyanate, *c*-$C_3H_5CH_2NCS$, dissolved in liquefied rare gases (Xe and Kr), have been carried out. The infrared spectra of the gas and solid, as well as the Raman spectrum of the liquid, have also been recorded from 3200 to 100 cm^{-1}. By analyzing six conformer pairs in xenon solutions, a standard enthalpy difference of 228 ± 23 cm^{-1} (2.73 ± 0.27 kJ·mol^{-1}) was obtained with the *gauche*−*cis* (the first designation indicates the orientation of the CNCS group with respect to the three-membered ring, the second designation indicates the relative orientation of the NCS group with respect to the bridging C−C bond) rotamer the more stable form, and it is also the only form present in polycrystalline solid. Given statistical weights of 2:1 for the *gauche*−*cis* and *cis*−*trans* forms (the only stable conformers predicted); the abundance of *cis*−*trans* conformer present at ambient temperature is 14 ± 2%. The potential surface describing the conformational interchange has been analyzed, and the corresponding two-dimensional Fourier coefficients were obtained. From MP2 ab initio calculations utilizing various basis sets with diffuse functions, the *gauche*−*cis* conformer is predicted to be more stable by 159−302 cm^{-1}, which is consistent with the experimental results. However, without diffuse functions, the conformational energy differences are nearly zero even with large basis sets. For calculations with density functional theory by the B3LYP method, basis sets without diffuse functions also predict smaller energy differences between the conformers, although not nearly as small as the MP2 results. A complete vibrational assignment for the *gauche*−*cis* conformer is proposed, and several fundamentals for the *cis*−*trans* conformer have been identified. The structural parameters, dipole moments, conformational stability, vibrational frequencies, and infrared and Raman intensities have been predicted from ab initio calculations and compared to the experimental values when applicable; the r_0 structural parameters are also estimated. The energies for the linear CNCS moiety were calculated. These experimental and theoretical results are compared to the corresponding quantities of some similar molecules.

Introduction

With the utilization of temperature-dependent conformational studies in rare gas solutions, the conformational stabilities of a series of monosubstituted methyl cyclopropane molecules have been studied in the past decade. These *c*-$C_3H_5CH_2X$ molecules, where X = F,[1] Cl,[2] Br,[2] CH_3,[3] C≡N,[4] and C≡CH,[5] have been found to exist in *cis* (X substituent over the three-membered ring with C_s molecular symmetry) and two equivalent *gauche* forms (X substituent rotated ∼±120° from the eclipsing position) in the fluid phases. A comparison of the results for this series of molecules proves to be interesting where all halogen substituents yield the gauche conformation more stable. The conformational enthalpy difference between *cis* and *gauche* forms in fluoromethyl cyclopropane was determined[1] to be 262 ± 26 cm^{-1} (3.13 ± 0.31 kJ·mol^{-1}) with the value for chloromethyl cyclopropane essentially the same where an enthalpy difference of 274 ± 21 cm^{-1} (3.28 ± 0.25 kJ·mol^{-1}) was reported.[2] However, the experimentally determined enthalpy difference for the bromide with a value of 383 ± 29 cm^{-1} (4.58 ± 0.35 kJ·mol^{-1})[2] is significantly larger than those for the two smaller halogen substituents. When the substituent is a methyl group (ethyl cyclopropane),which has a group radius comparable to that of the chlorine atom, few bands in the infrared spectrum were found for the less stable *cis* conformer, and the enthalpy difference was estimated to be ∼385 cm^{-1} (∼4.61 kJ·mol^{-1}).[3] Results from the halogen series seem to suggest that electronegativity and the size of the substituent are the determining factors in the conformational energy difference for monosubstituted methyl cyclopropane molecules. However, when the substituent is the cyano group, a pseudo halogen, the *gauche* conformer was determined[4] to be more stable by only 54 ± 4 cm^{-1} (0.65 ± 0.05 kJ·mol^{-1}). Additionally, in the case of ethynylmethyl cyclopropane, where the substituent is an ethynyl group (C≡CH), the conformational stability order was reversed with the *cis* conformer determined to be more stable by 147 ± 14 cm^{-1} (1.76 ± 0.17 kJ·mol^{-1}).[5] Results from these two substituents

* To whom correspondence should be addressed. Phone: 01 816-235-6038. Fax: 01 816-235-2290. E-mail: durigj@umkc.edu.
[†] University of Missouri−Kansas City.
[‡] Taken from the Ph.D. dissertation of C. Zheng, which will be submitted to the Department of Chemistry, University of Missouri−Kansas City.
[§] College of Charleston.
[||] University of Antwerp.

10.1021/jp0603740 CCC: $33.50
Published on Web 07/04/2006

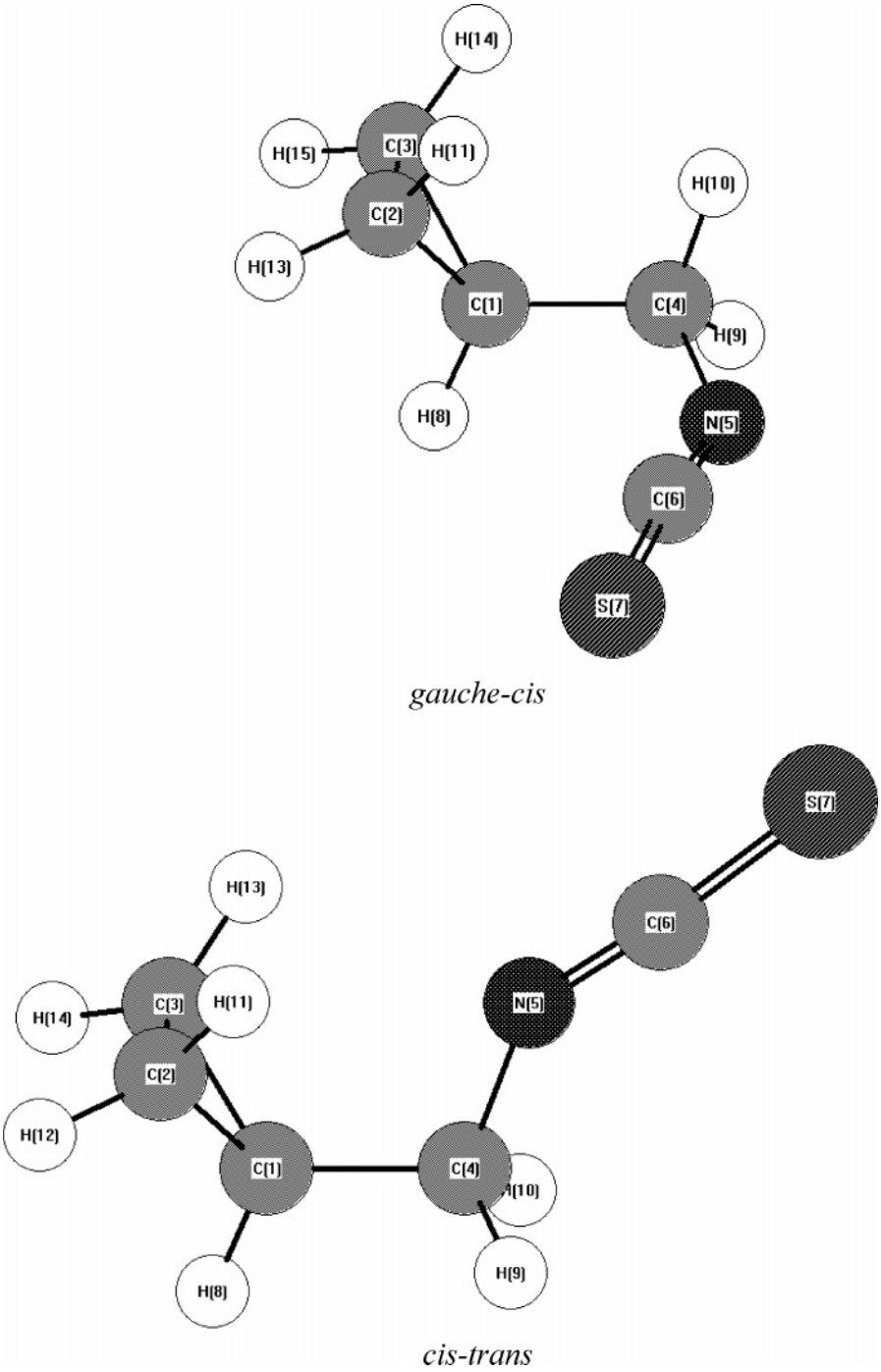

Figure 1. Stable *gauche*−*cis* and *cis*−*trans* conformers of cyclopropylmethyl isothiocyanate with atom numbering.

suggest that the orbital interaction between the three-membered ring and the triple bond leads to increased stability of the *cis* orientation, and this effect is dominant over the electronegativity and steric factors.

In an effort to gain further understanding into the factors determining conformational stabilities of the monosubstituted methylcyclopropane molecules, we have investigated the *gauche*/*cis* conformational equilibrium of cyclopropylmethyl isothiocyanate (Figure 1), where the substituent is an unsaturated isothiocyano group, by utilizing variable temperature infrared spectra of rare gas solutions. In addition to the relative positions (*gauche*- and *cis*-) of the CNCS group with respect to the three-membered ring (along the C−C bond), the relative orientation of the NCS group with respect to the bridging C−C bond gives rise to a second designation of conformations (along the C−N bond), i.e., *-cis* and *-trans*. To the best of our knowledge, there is no previous spectroscopic study on cyclopropylmethyl isothiocyanate. Thus, we have recorded infrared and/or Raman spectra of the sample in gas, liquid, and solid phases. The conformational stability, optimized geometry, force constants, vibrational frequencies, infrared intensities, Raman activities, and depolarization ratios have been obtained from ab initio calculations to compare with the experimental quantities when appropriate. The results of these vibrational, spectroscopic, and theoretical studies are reported herein.

Experimental Section

The cyclopropylmethyl isothiocyanate sample was purchased from Maybridge Chemical Co. (Cornwall, England) with a stated purity of 97+%. The sample was further purified with a low-

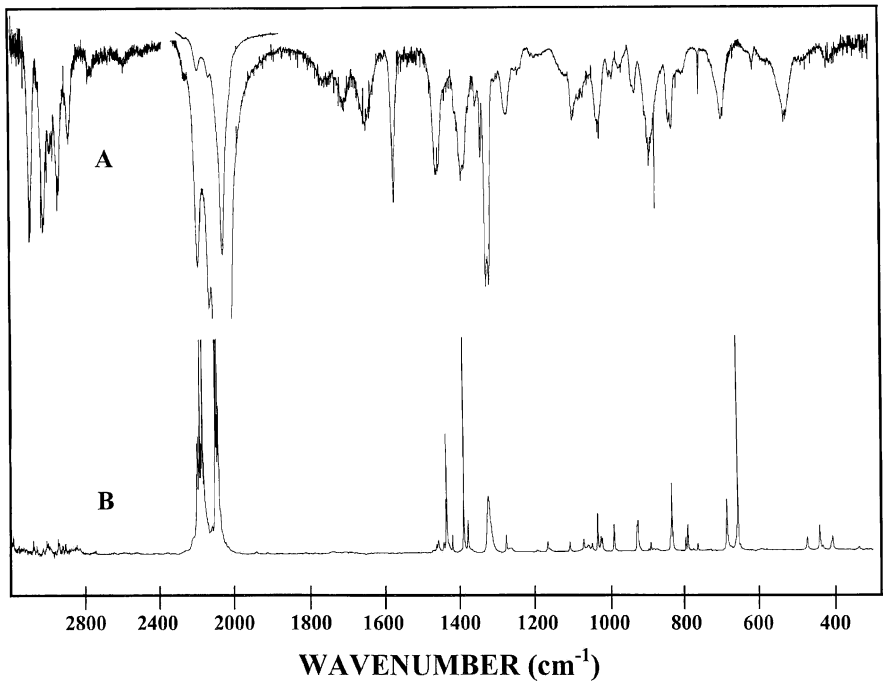

Figure 2. Infrared spectrum of (A) gaseous and (B) polycrystalline solid cyclopropylmethyl isothiocyanate.

pressure, low-temperature fractionation column, and the purity of the sample was checked by mass spectrometry. The purified sample was kept in the dark at low temperature until it was used.

The mid-infrared spectra (Figure 2) of the gas and the annealed solid from 3200 to 300 cm^{-1} were recorded on a Perkin-Elmer model 2000 Fourier transform spectrometer equipped with a Nichrome wire source, a Ge/CsI beam splitter, and a DTGS detector. The spectrum of the gas was obtained with the sample contained in a 10-cm cell equipped with CsI windows. Atmospheric water vapor was removed from the spectrometer chamber by purging with dry nitrogen. For the annealed solid, the spectrum was recorded by depositing a solid sample film onto a CsI substrate, which was cooled by boiling liquid nitrogen and housed in a vacuum cell fitted with CsI windows. The sample was annealed until no further change was observed in the spectrum. Interferograms obtained after 128 scans for the gas sample and reference, as well as 64 scans for the amorphous and annealed solid samples and references, were transformed by using a boxcar truncation function with theoretical resolutions of 0.5 and 1.0 cm^{-1}, respectively, for the gaseous and solid samples.

The mid-infrared spectra of the sample dissolved in liquefied xenon (Figure 3A) were recorded on a Bruker model IFS-66 Fourier interferometer equipped with a Globar source, a Ge/KBr beam splitter, and a DTGS detector. The spectra were recorded at variable temperatures ranging from −55 to −100 °C with 100 scans at a resolution of 1.0 cm^{-1}. The temperature studies in liquefied xenon were carried out in a specially designed cryostat cell, which is composed of a copper cell with a 4 cm path length and wedged silicon windows sealed to the cell with indium gaskets. The temperature was monitored by two Pt thermoresistors, and the cell was cooled by boiling liquid nitrogen. The complete cell was connected to a pressure manifold to allow for the filling and evacuation of the cell. After the cell was cooled to the desired temperature, a small amount of sample was condensed into the cell. Next, the pressure manifold and the cell were pressurized with xenon, which immediately started condensing in the cell, allowing the compound to dissolve.

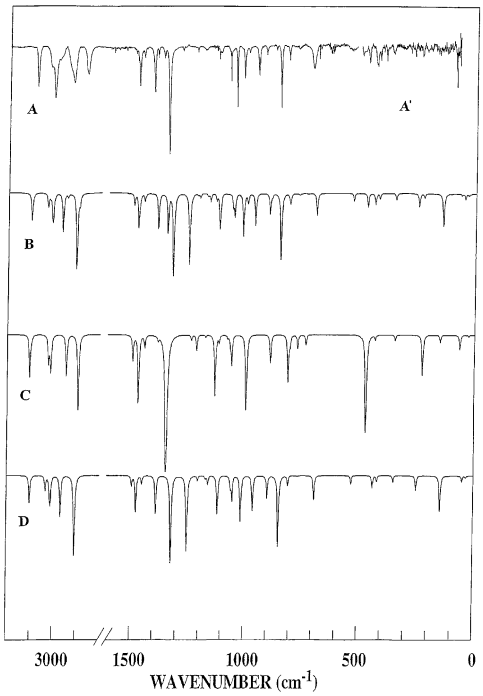

Figure 3. Infrared spectra of cyclopropylmethyl isothiocyanate: (A) xenon solution at −75 °C, (A′) far-infrared spectrum of Kr solution at −120 °C; (B) simulated spectrum of a mixture of the two conformers with ΔH of 228 cm^{-1} with the *gauche*−*cis* form more stable; (C) simulated spectrum for pure *cis*−*trans* form; (D) simulated spectrum for pure *gauche*−*cis* form.

The far-infrared spectra of the sample dissolved in liquid krypton were recorded on a Bruker model IFS 66 v/S Fourier transform spectrophotometer equipped with a Globar source, a 6.0 μm Mylar beam splitter, and a liquid helium cooled Si bolometer. The sample was contained in a 7-cm cell fitted with Si windows, and the sample was added as described for the

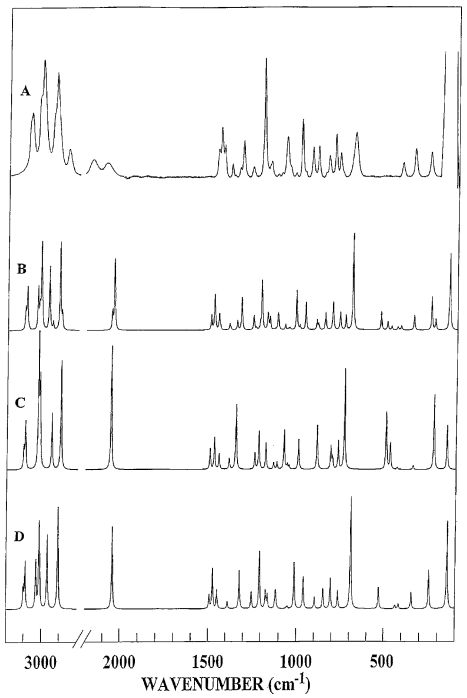

Figure 4. Raman spectra of cyclopropylmethyl isothiocyanate: (A) liquid at room temperature; (B) simulated spectrum of a mixture of the two conformers with ΔH of 228 cm^{-1} with the *gauche*−*cis* form more stable; (C) simulated spectrum for pure *cis*−*trans* form; (D) simulated spectrum for pure *gauche*−*cis* form.

mid-infrared studies. For all spectra, 250 interferograms were collected at 0.5 cm^{-1} resolution, averaged, and transformed with a Blackman−Harris three-term function, and a typical spectrum is shown in Figure 3A′.

The Raman spectrum of liquid cyclopropylmethyl isothiocyanate from 3200 to 150 cm^{-1} was recorded on a Holospec (Kaiser Optical Systems Inc., Ann Arbor, MI) spectrophotometer equipped with a Coherent Ti:sapphire laser pumped by Coherent argon ion laser and a streak camera system consisting of a liquid nitrogen-cooled CCD array for detection. The excitation wavelength was 752 nm, and the average power incident on the sample was 600 mW. Two 752-nm holographic notch filters were used to remove the excitation light. In the spectral range from 150 to 1800 cm^{-1}, the camera exposure time was set to be 2 s and a total of 10 spectra were taken. After the grating change for the 1800−3200 cm^{-1} range, the camera exposure time was set to be 4 s and a total of seven spectra were taken; these spectra were then averaged to obtain the experimental spectrum shown in Figure 4A. The liquid sample was sealed in a glass capillary, and the spectrum was recorded at 25 °C. Raman shifts are expected to be accurate to ±2 cm^{-1}.

Ab Initio Calculations

The LCAO-MO−SCF calculations were performed with the Gaussian-03 program[6] by using Gaussian-type basis functions. The energy minima with respect to nuclear coordinates were obtained by simultaneous relaxation of all geometric parameters consistent with symmetry restrictions using the gradient method of Pulay.[7] Results from frequency calculations suggest that the *gauche*−*cis* and *cis*−*trans* are the only stable conformations (Figure 1) corresponding to local minima on the potential surface whereas the *gauche*−*trans* and *cis*−*cis* forms gave one imaginary frequency, indicating that they are first-order saddle points. The predicted wavenumbers of the fundamentals of the stable *gauche*−*cis* and *cis*−*trans* conformers are listed in Tables 1 and 2, respectively, along with the observed values. A number of basis sets starting from 6-31G(d), and increasing to 6-311+G-(2df,2pd), were employed at the level of Hartree−Fock, Møller−Plesset perturbation theory to the second order (MP2(full)) as well as hybrid density functional theory by the B3LYP method, to obtain energy differences between the two stable conformers as well as relative energies of first-order saddle points (Table 3). It is interesting to note that MP2(full)/6-311G(2d,2p) and MP2(full)/6-311G(2df,2pd) calculations predict the *cis*−*cis* form more stable than the *gauche*−*cis* form. However, frequency calculations at the same levels result in one imaginary frequency for the *cis*−*cis* form, indicating that it is a first-order saddle point, not a stable conformer. Such discrepancy at certain levels of calculation in which the form with the lowest energy is predicted, at the same time, to be a first-order saddle point, can also be found in cyclopentyl germane[8] where MP2(full)/6-31G-(d) and MP2(full)/6-311+G(d,p) levels predict the *twist* form having the lowest energy yet with one imaginary frequency. These discrepancies are believed to arise from the mismatch of the electron correlation and the basis set size, or more strictly, insufficient treatment of such. From all levels of calculation conducted in the present investigation, the *gauche*−*cis* conformer is always predicted to be more stable than the *cis*−*trans* form. However, there are large variations in the predicted conformational energy difference depending on whether diffuse functions are included. The MP2 calculations with diffuse functions predict the *gauche*−*cis* conformer to be more stable by a low value of 159 cm^{-1} [MP2(full)/6-311+G(2d,2p)] to a high value of 302 cm^{-1} [MP2(full)/6-311+G(d,p)]. Calculations without diffuse functions predict much smaller conformational energy differences, with the *gauche*−*cis* form having nearly the same energy (energy difference only 9 cm^{-1}) as the *cis*−*trans* form at the MP2(full)/6-311G(2d,2p) level. Similar dependence on the inclusion of diffuse functions is also predicted, although to a lesser extent, from hybrid density functional theory by the B3LYP method. The significant discrepancies with the predicted results indicate that the theoretical calculations at the levels studied cannot be confidently relied on to provide an accurate energy difference between the two conformers.

To obtain a more complete description of the nuclear motions involved in the vibrational fundamentals of cyclopropylmethyl isothiocyanate, we have carried out normal coordinate analyses. The force fields in Cartesian coordinates were calculated by the Gaussian-03 program at the MP2(full)/6-31G(d) level. The internal coordinates used to calculate the **G** and **B** matrixes are listed along with the structural parameters in Table 4, and the atom numbering is shown in Figure 1. By using the **B** matrix, the force field in Cartesian coordinates was converted to a force field in internal coordinates[9] in which the pure ab initio vibrational frequencies were reproduced. Subsequently, scaling factors of 0.88 for the CH stretches, 1.0 for heavy atom bends and torsions, and 0.90 for all other modes were used, along with the geometric average of scaling factors for interaction force constants, to obtain the fixed scaled force field (Table 1S, Supporting Information) and the resultant wavenumbers. A set of symmetry coordinates was used (Table 2S, Supporting Information) to determine the corresponding potential energy distributions (PEDs), which are listed Tables 1 and 2.

To identify the fundamental vibrations for the *gauche*−*cis* and *cis*−*trans* conformers of cyclopropylmethyl isothiocyanate, the infrared spectra were predicted using fixed scaled frequencies. Infrared intensities determined from MP2(full)/6-31G(d) calculations were calculated on the basis of the dipole moment

TABLE 1: Observed and Calculated Frequencies (cm^{-1}) for *gauche−cis* Cyclopropylmethyl Isothiocyanate

vib. no.	fundamental	ab initio[a]	fixed scaled[b]	IR int.[c]	Raman act.[d]	dp ratio	IR gas	IR Xe[e]	Raman liquid	IR solid	PED.[f]	A[g]	B[g]	C[g]
ν_1	rCH_2 antisymmetric stretch	3306	3101	8.6	35.2	0.58	3097	3086	3087	3084	$98S_1$	10	24	66
ν_2	rCH_2 antisymmetric stretch	3295	3091	0.3	73.2	0.74	3091	3073	3078	3070	$98S_2$	16	0	84
ν_3	CH stretch	3230	3030	4.5	71.9	0.24	3034	3028	3031	3031	$97S_3$	1	7	92
ν_4	rCH_2 symmetric stretch	3210	3012	4.1	121.5	0.05	3023	3012	3012	3011	$97S_4$	30	19	51
ν_5	rCH_2 symmetric stretch	3206	3008	8.3	28.4	0.55	3009	2992	3012	2994	$98S_5$	81	19	0
ν_6	CH_2 antisymmetric stretch	3162	2966	13.8	108.4	0.57	2945	2929	2935	2926	$90S_6$	8	67	25
ν_7	CH_2 symmetric stretch	3098	2906	33.6	144.9	0.08	2884	2871	2873	2877	$91S_7$	50	33	17
ν_8	C═N stretch	2154	2043	991.4	67.2	0.30	2062	2071	2093	2102	$81S_8$, $13S_{28}$	82	18	0
ν_9	rCH_2 deformation	1573	1493	2.9	7.3	0.74		1465	1465	1459	$74S_9$, $15S_{15}$	28	6	66
ν_{10}	CH_2 deformation	1553	1474	11.9	20.7	0.58	1455	1450	1449	1437	$91S_{10}$	84	1	15
ν_{11}	rCH_2 deformation	1527	1448	2.5	9.4	0.66		1429	1431	1421	$99S_{11}$	59	41	0
ν_{12}	CH in-plane bend	1463	1388	12.7	3.4	0.73	1394	1386	1385	1391	$38S_{12}$, $14S_9$, $13S_{26}$, $13S_{15}$, $12S_{13}$	94	0	6
ν_{13}	CH_2 wag	1391	1321	38.4	17.1	0.53	1329	1322	1324	1325	$78S_{13}$, $11S_{14}$	98	0	2
ν_{14}	CH_2 twist	1317	1251	30.6	7.0	0.72	1273	1262	1267	1278	$62S_{14}$, $13S_{17}$	82	17	1
ν_{15}	ring breathing	1270	1205	1.4	22.8	0.22		1198	1202	1195	$52S_{15}$, $27S_{12}$	8	90	2
ν_{16}	rCH_2 twist	1234	1171	0.9	6.8	0.73		1167	1171	1168	$39S_{16}$, $46S_{25}$, $12S_{19}$	23	71	6
ν_{17}	rCH_2 twist	1218	1160	2.6	5.4	0.21		1161	1163	1163	$15S_{17}$, $22S_{22}$, $16S_{26}$, $13S_{12}$	67	14	19
ν_{18}	C−N stretch	1175	1117	10.6	4.3	0.35	1097	1102	1105	1109	$37S_{18}$, $24S_{28}$, $22S_{19}$	90	10	0
ν_{19}	CH out-of-plane bend	1173	1114	4.1	4.4	0.38	1093	1096	1105	1109	$41S_{19}$, $29S_{16}$, $15S_{18}$	0	92	8
ν_{20}	rCH_2 wag	1114	1057	3.2	0.4	0.34	1054	1051		1049	$96S_{20}$	84	13	3
ν_{21}	rCH_2 wag	1104	1050	7.6	0.8	0.28	1028	1024	1026	1026	$84S_{21}$, $11S_{23}$	1	49	50
ν_{22}	CH_2 rock	1053	1012	15.7	14.7	0.40	994	991	992	991	$18S_{22}$, $19S_{24}$, $14S_{26}$, $11S_{23}$	2	95	3
ν_{23}	ring deformation	991	960	11.4	9.6	0.75	929	930	931	927	$31S_{23}$, $33S_{24}$	39	41	20
ν_{24}	ring deformation	941	897	6.9	3.2	0.49	892	896	898	892	$10S_{24}$, $38S_{22}$, $26S_{27}$	93	0	7
ν_{25}	rCH_2 rock	882	848	27.9	5.1	0.62	835	833	837	837	$18S_{25}$, $29S_{24}$, $13S_{23}$, $12S_{19}$	78	20	2
ν_{26}	C−C stretch	842	806	2.8	7.3	0.74	798	796	800	794	$14S_{26}$, $24S_{23}$, $17S_{25}$	2	0	98
ν_{27}	rCH_2 rock	804	764	0.3	4.1	0.75	758	755	773	768	$45S_{27}$, $44S_{17}$	70	2	28
ν_{28}	C═S stretch	725	691	33.1	22.1	0.28	699	691	684	691	$43S_{28}$, $24S_{18}$, $18S_8$	97	2	1
ν_{29}	CCN bend	534	529	43.6	3.0	0.20	526	517		476	$23S_{29}$, $47S_{31}$	44	56	0
ν_{30}	NCS out-of-plane bend	436	435	3.7	0.4	0.75	447	445		443	$77S_{30}$, $13S_{31}$	54	0	46
ν_{31}	NCS in-plane bend	420	416	1.7	0.5	0.37	408	(409)	407	408	$28S_{31}$, $19S_{30}$, $15S_{33}$, $12S_{29}$	54	33	13
ν_{32}	ring-C in-plane bend	353	346	1.9	1.3	0.19		(340)	345	338	$73S_{32}$	53	47	0
ν_{33}	ring-C out-of-plane bend	248	247	4.3	1.8	0.72		(248)	255	254	$57S_{33}$, $27S_{29}$	16	56	28
ν_{34}	ring torsion	144	144	11.6	2.2	0.74		(142)			$62S_{34}$, $27S_{35}$	53	29	18
ν_{35}	CNC bend	50	50	1.7	4.2	0.66					$61S_{35}$, $25S_{34}$	91	7	2
ν_{36}	C−N torsion	34	34	0.6	2.6	0.75					$93S_{36}$	3	0	97

[a] MP2/6-31G(d) predicted values. [b] MP2/6-31G(d) fixed scaled frequencies with factors of 0.88 for CH stretches, 1.0 for heavy atom bends, 1.0 for torsion, and 0.90 for all other modes. [c] Scaled infrared intensities in km/mol from MP2/6-31G(d). [d] Scaled Raman activities in $Å^4$/amu from MP2/6-31G(d). [e] Frequencies from mid-IR spectrum of Xe solution at −75 °C; numbers in parentheses are from far-IR spectrum of Kr solution at −120 °C. [f] Calculated with MP2/6-31G(d), and contributions of less than 10% are omitted. [g] A, B, and *C* values in the last three columns are percentage infrared band contours.

derivatives with respect to Cartesian coordinates. The derivatives were transformed with respect to normal coordinates by $(\partial\mu_u/\partial Q_i) = \sum_j (\partial\mu_u/\partial X_j)\, L_{ij}$, where Q_i is the ith normal coordinate, X_j is the jth Cartesian displacement coordinate, and L_{ij} is the transformation matrix between the Cartesian displacement coordinates and the normal coordinates. The infrared intensities were then calculated by $(N\pi)/(3c^2)\,[(\partial\mu_x/\partial Q_i)^2 + (\partial\mu_y/\partial Q_i)^2 + (\partial\mu_z/\partial Q_i)^2]$. In Figure 3D,C, the simulated infrared spectra of the pure *gauche−cis* and *cis−trans* conformers, respectively, are shown. The simulated spectra, calculated for −75 °C, of a mixture of two conformers with a ΔH of 228 cm^{-1} (experimental value), is shown in Figure 3B, and it should be compared to the experimental spectrum of the xenon solution at −75 °C (Figure 3A). The predicted spectrum is in remarkably good agreement with the experimental spectrum, which indicates the utility of the scaled predicted data in distinguishing the fundamentals for the two conformers. One exception is the ν_{14} (CH_2 twist) band of the *gauche−cis* conformer, the observed intensity of which is significantly smaller than the predicted value. Also, the ν_{28} (C═S stretch) band of the *gauche−cis* conformer is significantly broader in the spectrum of xenon solution compared to the one collected for the gas phase, probably due to the sample's association with the xenon solvent.

To further support the vibrational assignments, we have simulated the Raman spectra from the *ab* initio MP2(full)/6-31G(d) results. The evaluation of Raman activity by using the analytical gradient methods has been developed.[10,11] The activity S_j can be expressed as: $S_j = g_j\,(45\alpha_j^2 + 7\beta_j^2)$, where g_j is the degeneracy of the vibrational mode j, α_j is the derivative of the isotropic polarizability, and β_j is that of the anisotropic polarizability. To obtain the polarized Raman scattering cross sections, the polarizabilities are incorporated into S_j by multiplying S_j with $(1-\rho_j)/(1+\rho_j)$, where ρ_j is the depolarization ratio of the jth normal mode. The Raman scattering cross sections and calculated wavenumbers obtained from the Gaussian 03 program were used together with a Lorentzian function to obtain the simulated Raman spectra.

The simulated Raman spectra of the pure *gauche−cis* and *cis−trans* conformers are shown in Figure 4D,C, respectively. The simulated Raman spectra, calculated for 25 °C of a mixture of two conformers with a ΔH of 228 cm^{-1}, is shown in Figure 4B. The experimental Raman spectrum of the liquid is shown in Figure 4A for comparison, and the agreement is considered satisfactory, but not nearly as good as that of the infrared spectrum, probably due, in part, to the significant extent of intermolecular association in the liquid phase. Additionally, the

TABLE 2: Observed and Calculated Frequencies (cm^{-1}) for *cis*−*trans* Cyclopropylmethyl Isothiocyanate

	vib. no.	fundamental	ab initio[a]	fixed scaled[b]	IR int.[c]	Raman act.[d]	dp ratio	IR gas	IR Xe[e]	Raman liquid	PED.[f]	A[g]	B[g]	C[g]
A′	ν_1	rCH_2 antisymmetric stretch	3309	3104	14.4	33.0	0.54				$100S_1$	100	0	−
A″	ν_2	rCH_2 antisymmetric stretch	3299	3095	0.6	75.3	0.75				$100S_2$	−	−	100
A′	ν_3	CH stretch	3220	3021	8.6	196.2	0.16				$85S_3$, $14S_4$	72	28	−
A′	ν_4	rCH_2 symmetric stretch	3212	3013	5.3	107.2	0.14				$86S_4$, $14S_3$	0	100	−
A″	ν_5	rCH_2 symmetric stretch	3210	3011	8.2	24.1	0.75				$100S_5$	−	−	100
A″	ν_6	CH_2 antisymmetric stretch	3140	2945	14.1	81.7	0.75				$100S_6$	−	−	100
A′	ν_7	CH_2 symmetric stretch	3085	2894	30.8	154.1	0.05				$100S_7$	10	90	−
A′	ν_8	C═N stretch	2166	2055	1090.4	101.9	0.30				$81S_8$, $13S_{28}$	96	4	−
A′	ν_9	rCH_2 deformation	1574	1493	8.0	10.8	0.56				$71S_9$, $19S_{15}$	93	7	−
A′	ν_{10}	CH_2 deformation	1547	1468	26.7	16.2	0.62				$99S_{10}$	100	0	−
A″	ν_{11}	rCH_2 deformation	1519	1441	3.6	7.7	0.75				$100S_{11}$	−	−	100
A′	ν_{12}	CH in-plane bend	1457	1383	1.2	5.0	0.52		1370	1373	$40S_{12}$, $23S_9$, $13S_{15}$, $13S_{26}$	23	77	−
A′	ν_{13}	CH_2 wag	1417	1346	148.6	29.8	0.42	1342	1343	1342	$81S_{13}$	99	1	−
A″	ν_{14}	CH_2 twist	1302	1237	1.6	6.6	0.75		1254	1257	$92S_{14}$	−	−	100
A′	ν_{15}	ring breathing	1279	1214	4.8	15.3	0.38		1207		$44S_{15}$, $28S_{12}$, $11S_{17}$	95	5	−
A″	ν_{16}	rCH_2 twist	1238	1175	0.7	10.1	0.75			1180	$45S_{16}$, $45S_{25}$	−	−	100
A′	ν_{17}	rCH_2 twist	1131	1075	1.0	13.5	0.08			1076	$19S_{17}$, $21S_{28}$, $19S_{18}$, $15S_{12}$, $13S_{27}$	24	76	−
A′	ν_{18}	C−N stretch	1189	1132	22.9	2.4	0.32		1125	1125	$32S_{18}$, $15S_{28}$, $12S_{13}$, $10S_{17}$	88	12	−
A″	ν_{19}	CH out-of-plane bend	1174	1114	2.2	2.6	0.75				$63S_{19}$, $29S_{16}$	−	−	100
A″	ν_{20}	rCH_2 wag	1120	1063	2.6	0.3	0.75				$94S_{20}$	−	−	100
A′	ν_{21}	rCH_2 wag	1110	1057	9.5	1.6	0.26				$77S_{21}$, $14S_{26}$	27	73	−
A″	ν_{22}	CH_2 rock	1091	1047	0.01	1.2	0.75				$56S_{22}$, $30S_{24}$, $11S_{33}$	−	−	100
A′	ν_{23}	ring deformation	1035	993	30.8	9.3	0.47	971	971	971	$35S_{23}$, $22S_{26}$, $18S_{21}$	42	58	−
A″	ν_{24}	ring deformation	916	888	9.0	11.9	0.75	857	854	854	$75S_{24}$, $18S_{22}$	−	−	100
A″	ν_{25}	rCH_2 rock	844	801	2.7	2.9	0.75				$41S_{25}$, $24S_{19}$, $19S_{16}$, $15S_{24}$	−	−	100
A′	ν_{26}	C−C stretch	848	810	16.3	5.4	0.66	819	811	818	$19S_{26}$, $40S_{27}$, $16S_{23}$, $12S_{28}$	72	28	−
A′	ν_{27}	rCH_2 rock	804	768	4.1	6.3	0.70				$32S_{27}$, $33S_{17}$, $20S_{23}$, $12S_{26}$	58	42	−
A′	ν_{28}	C═S stretch	760	732	3.0	21.3	0.19		728		$17S_{28}$, $23S_{29}$, $16S_{18}$, $11S_{23}$	57	43	−
A′	ν_{29}	CCN bend	503	491	0.2	7.2	0.40	474	473		$12S_{29}$, $30S_{32}$, $29S_{31}$, $12S_{18}$	3	97	−
A″	ν_{30}	NCS out-of-plane bend	429	429	1.5	0.2	0.75				$97S_{30}$	−	−	100
A′	ν_{31}	NCS in-plane bend	472	468	47.5	3.1	0.53	458	453		$64S_{31}$	99	1	−
A′	ν_{32}	ring-C in-plane bend	228	225	13.7	3.0	0.71		(216)		$45S_{32}$, $36S_{29}$	100	0	−
A″	ν_{33}	ring-C out-of-plane bend	346	343	1.8	0.3	0.75		(334)		$86S_{33}$	−	−	100
A″	ν_{34}	ring torsion	150	150	2.2	0.9	0.75		(149)		$98S_{34}$	−	−	100
A′	ν_{35}	CNC bend	66	66	4.4	6.1	0.73				$84S_{35}$	96	4	−
A″	ν_{36}	C−N torsion	27	27	0.5	6.0	0.75				$100S_{36}$	−	−	100

[a] MP2/6-31G(d) predicted values. [b] MP2/6-31G(d) fixed scaled frequencies with factors of 0.88 for CH stretches, 1.0 for heavy atom bends, 1.0 for torsion, and 0.90 for all other modes. [c] Scaled infrared intensities in km/mol from MP2/6-31G(d). [d] Scaled Raman activities in $Å^4$/amu from MP2/6-31G(d). [e] Frequencies from mid-IR spectrum of Xe solution at −75 °C; numbers in parentheses are from far-IR spectrum of Kr solution at −120 °C. [f] Calculated with MP2/6-31G(d), and contributions of less than 10% are omitted. [g] *A*, *B*, and *C* values in the last three columns are percentage infrared band contours.

ab initio predictions of Raman line intensities are not usually as good as the predictions of the corresponding infrared intensities.

Vibrational Assignment

To determine the relative conformational stabilities of the two conformers of cyclopropylmethyl isothiocyanate, it is necessary first to assign bands to each conformer. However, it is a daunting task to provide a complete vibrational assignment because most fundamental vibrations of the two conformers have nearly the same predicted force constants and consequently frequencies, with the largest difference arising from skeletal bending modes. Identification of the bands due to a second conformer in the spectra of the fluid phases, as compared with bands arising from a single conformer in the polycrystalline phase, provides further support for correct assignments. Because of the relatively large and nearly equal moments of inertia between the two conformations of cyclopropylmethyl isothiocyanate, the predicted gas phase infrared band contours differ only slightly between those for the *cis*−*trans* and *gauche*−*cis* forms, with that of the *cis*−*trans* form exhibiting more pronounced fine rotational structure for B- and C- type envelopes as shown in Figure 5. Because the *cis*−*trans* conformer has C_s symmetry, with the symmetry plane coinciding with that of *ab* figure axes, the gas-phase A′ vibrational modes are expected to exhibit A/B hybrid band envelopes and all A″ modes give rise to C-type envelopes, whereas the fundamentals of the *gauche*−*cis* form are expected to give rise to A/B/C hybrid contours.

Group frequencies for the monosubstituted three-membered ring have been well characterized and similarly for those of the −NCS group. Therefore, by comparing these data along with the ab initio predicted infrared and Raman intensities as well as gas phase infrared band envelopes, a reasonably confident vibrational assignment has been provided for the fundamental modes for the *gauche*−*cis* form and many of those for the *cis*−*trans* conformer (Tables 1 and 2). The low-frequency heavy atom bends and torsions are very sensitive to skeletal structural differences between the two conformers. The predicted frequencies of some of these modes demonstrate significant differences between the *gauche*−*cis* and the *cis*−*trans* forms. For example,

TABLE 3: Calculated Energies (Hartree) for the Most Stable *gauche*−*cis* Conformation and Energy Differences (cm^{-1}) for the Less Stable *cis*−*trans* Conformation as Well as the *gauche*−*trans* and *cis*−*cis* First-Order Saddle Points of Cyclopropylmethyl Isothiocyanate[a]

method/basis set	*gauche*−*cis*	Δ*E*	*cis*−*trans*	Δ*E*	*gauche*−*trans*	Δ*E*	*cis*−*cis*	Δ*E*
RHF/6-31G(d)	−645.336283[b]	0	−645.334677[b]	353	−645.336283[b]	0	−645.334677[b]	353
RHF/6-31+G(d)	−645.340913[b]	0	−645.339179[b]	380	−645.340913[b]	0	−645.339179[b]	380
MP2/6-31G(d)	−646.299120	0	−646.298605	113	−646.297886	271	−646.298222	197
MP2/6-31+G(d)	−646.315440	0	−646.314326	245	−	−	−646.314191	274
MP2/6-311G(d,p)	−646.660886	0	−646.660488	87	−646.659424	321	−646.660371	113
MP2/6-311+G(d,p)	−646.670532	0	−646.669157	302	−	−	−646.669428	242
MP2/6-311G(2d,2p)	−646.757118	0	−646.757077	9	−	−	−646.757197	−17
MP2/6-311+G(2d,2p)	−646.764101	0	−646.763379	159	−	−	−646.763742	79
MP2/6-311G(2df,2pd)	−646.882278	0	−646.882132	32	−	−	−646.882761	−106
MP2/6-311+G(2df,2pd)	−646.888164	0	−646.887267	197	−	−	−646.888114	11
B3LYP/6-31G(d)	−647.648258	0	−647.647082	258	−647.647509	164	−647.646359	417
B3LYP/6-31+G(d)	−647.657115	0	−647.655878	272	−647.656632	106	−	−
B3LYP/6-311G(d,p)	−647.739130	0	−647.738300	182	−647.738524	133	−	−
B3LYP/6-311+G(d,p)	−647.743090	0	−647.742084	221	−647.742703	85	−	−
B3LYP/6-311G(2d,2p)	−647.750695	0	−647.750044	143	−647.750232	102	−647.748935	386
B3LYP/6-311+G(2d,2p)	−647.754269	0	−647.753089	259	−647.753823	98	−647.752059	485
B3LYP/6-311G(2df,2pd)	−647.763186	0	−647.762435	165	−647.762725	101	−	−
B3LYP/6-311+G(2df,2pd)	−647.766371	0	−647.765174	263	−647.765959	90	−647.764422	428

[a] Entries with bars cannot be optimized. [b] RHF/6-31G(d) and RHF/6-31+G(d) calculations result in linear CNCS structure.

the CCN bend (ν_{29}) is predicted at 529 cm^{-1} for the *gauche*−*cis* form whereas the *cis*−*trans* fundamental is predicted 38 cm^{-1} lower at 491 cm^{-1}. Two distinctive bands, the stronger one at 517 cm^{-1} and the weaker one at 473 cm^{-1}, were observed in the spectra of the noble gas (Kr and Xe) solutions. The gas-phase band envelope predicted for the *gauche*−*cis* form is a mixture of 56% B-type and 44% A-type, whereas the one for the *cis*−*trans* form is 97% B-type. Thus, the Q-branch at 526 cm^{-1} in the spectrum of the gas is assigned to the *gauche*−*cis* conformer, and the much weaker B-type minimum at 473 cm^{-1} is assigned to the *cis*−*trans* form. Another example involving large differences in predicted frequencies is the NCS in-plane bend (ν_{31}). The fundamental for the *gauche*−*cis* conformer is predicted at 416 cm^{-1} with an intensity of 1.7 km·mol^{-1}, whereas the corresponding mode for the *cis*−*trans* conformer is predicted 52 cm^{-1} higher at 468 cm^{-1} with an intensity of 47.5 km·mol^{-1}, which is 28 times stronger than the predicted value for the *gauche*−*cis* form. These large differences in predicted frequencies and intensities arise from the significantly different NCS orientations between the *gauche*−*cis* and the *cis*−*trans* forms. Again, two pronounced bands at 409 and 453 cm^{-1} are observed in the spectra of noble gas (Kr and Xe) solutions, whereas in the IR spectrum of the gas, a Q-branch is observed at 408 cm^{-1} and a weaker band with a sharp Q-branch is observed at 458 cm^{-1}. Because of the large difference in predicted frequencies for these fundamentals between the conformations, there is no question that the higher frequency band must be assigned to the *cis*−*trans* form. On the basis of the predicted intensities with the experimental lower frequency band more intense, a relatively large enthalpy difference is expected between the two conformers with the *gauche*−*cis* form more stable. Only one of these bands is observed at 408 cm^{-1} in the IR spectrum of the annealed solid, which suggests the *gauche*−*cis* form is the only conformation present in the polycrystalline solid state of cyclopropylmethyl isothiocyanate.

In the crowded "fingerprint" region, particularly for the spectral region between 700 and 1400 cm^{-1}, many of the assignments were strongly dependent on the ab initio predictions. Also, the descriptions provided in some cases are more for bookkeeping than for giving the exact atomic motions involved because the potential energy distribution analysis showed that a number of vibrations have three or four significant symmetry coordinate contributions. Thus, extensive mixing in the spectral regions is predicted for both the *gauche*−*cis* and *cis*−*trans* conformers. For the *gauche*−*cis* form, four fundamental vibrations have contributions from four or five different symmetry coordinates with the maximum contribution from any one of them in the mid-thirty percent range (Table 1), whereas for the *cis*−*trans* form, seven fundamental modes involve four or five symmetry coordinates to a significant extent (Table 2). The largest mixings can be attributed to three ring-CH bending modes, namely: ν_{12}, CH in-plane bend; ν_{17}, (ring)CH_2 twist; and ν_{25}, (ring)CH_2 rock.

The assignments for the carbon−hydrogen stretches are rather straightforward, where the C−H modes of the ring have significantly higher frequencies than those for the methylene −CH_2(NCS) group. There is little separation between the two ring-CH_2 antisymmetric stretches, and the same is true for the two corresponding symmetric modes; however, the two antisymmetric CH_2 stretches of the three-membered ring are approximately 80 cm^{-1} higher than the symmetric stretches in both predicted and observed frequencies.

Conformational Stability

To determine the enthalpy difference between the two conformers, the mid-infrared spectra of cyclopropylmethyl isothiocyanate dissolved in liquefied xenon as a function of temperature from −55 to −100 °C were recorded. Only small interactions are expected to occur between the dissolved sample and the surrounding xenon atoms, and consequently, only small frequency shifts are anticipated when passing from the gas phase to the liquefied noble gas solutions.[14−16] A significant advantage of this study is that the conformer bands are better resolved in comparison with those in the infrared spectrum of the gas. From ab initio calculations, the dipole moments of the two conformers are predicted to have similar values and the molecular sizes of the two rotamers are nearly the same, so the Δ*H* value obtained from the temperature-dependent FT-IR study is expected to be close to that for the gas.[14−16]

A careful comparison between the infrared spectrum of the xenon solutions and that of the annealed solid revealed the disappearance of several bands in the polycrystalline solid, and these bands can be identified as due to the *cis*−*trans* conformer in the fluid phases. Two pronounced bands in the spectra of the xenon solutions at 1343 cm^{-1} [CH_2 wag (ν_{13})] and 1370 cm^{-1} [CH in-plane bend (ν_{12})] disappear in the spectrum of the solid (Figure 2). Both bands are well separated from the

TABLE 4: Structural Parameters (Å and Degrees), Rotational Constants (MHz), and Dipole Moments (Debye) for *gauche*−*cis* and *cis*−*trans* Rotamers of Cyclopropylmethyl Isothiocyanate

	internal coordinates	MP2(full)/6-311+G(d,p)		estimated r_0	
		gauche−*cis*	*cis*−*trans*	*gauche*−*cis*	*cis*−*trans*
$r(C_1C_2)$	R_1	1.505	1.504	1.507(5)	1.508(5)
$r(C_1C_3)$	R_2	1.508	1.504	1.512(5)	1.508(5)
$r(C_2C_3)$	R_3	1.511	1.513	1.513(5)	1.516(5)
$r(C_1C_4)$	R_4	1.505	1.510	1.507(5)	1.513(5)
$r(C_4N_5)$	R_5	1.446	1.439	1.443(5)	1.437(5)
$r(N_5C_6)$	R_6	1.210	1.208	1.202(5)	1.200(5)
$r(C_6S_7)$	R_7	1.577	1.576	1.578(5)	1.577(5)
$r(C_1H_8)$	r_5	1.086	1.086	1.086(2)	1.086(2)
$r(C_2H_{11})$	r_1	1.085	1.084	1.085(2)	1.084(2)
$r(C_2H_{12})$	r_2	1.083	1.083	1.083(2)	1.083(2)
$r(C_3H_{13})$	r_3	1.085	1.084	1.085(2)	1.084(2)
$r(C_3H_{14})$	r_4	1.083	1.083	1.083(2)	1.083(2)
$r(C_4H_9)$	r_6	1.094	1.097	1.094(2)	1.097(2)
$r(C_4H_{10})$	r_7	1.096	1.097	1.096(2)	1.097(2)
$\angle C_2C_1C_3$		60.2	60.4	60.2(3)	60.3(3)
$\angle C_2C_1C_4$	ϵ_1	118.4	120.2	117.2(5)	120.0(5)
$\angle C_3C_1C_4$	ϵ_2	119.0	120.2	119.8(5)	120.0(5)
$\angle C_1C_4N_5$	δ	111.2	110.9	111.4(5)	111.1(5)
$\angle C_4N_5C_6$	φ	140.1	144.0	140.1(5)	144.0(5)
$\angle N_5C_6S_7$	θ	174.9	174.7	175.1(5)	174.9(5)
$\angle C_1C_2H_{11}$	α_1	117.2	117.2	117.2(5)	117.2(5)
$\angle C_1C_2H_{12}$	α_2	117.9	117.9	117.9(5)	117.9(5)
$\angle C_3C_2H_{11}$	β_1	117.4	116.7	117.4(5)	116.7(5)
$\angle C_3C_2H_{12}$	β_2	118.2	118.2	118.2(5)	118.2(5)
$\angle C_1C_3H_{13}$	α_3	117.5	117.2	117.5(5)	117.2(5)
$\angle C_1C_3H_{14}$	α_4	117.8	117.9	117.8(5)	117.9(5)
$\angle C_2C_3H_{13}$	β_3	117.5	116.7	117.5(5)	116.7(5)
$\angle C_2C_3H_{14}$	β_4	118.2	118.2	118.2(5)	118.2(5)
$\angle H_{11}C_2H_{12}$	γ	115.1	115.6	115.1(5)	115.6(5)
$\angle H_{13}C_3H_{14}$	γ'	115.0	115.6	115.0(5)	115.6(5)
$\angle C_2C_1H_8$	σ_1	116.7	116.6	116.7(5)	116.6(5)
$\angle C_3C_1H_8$	σ_2	117.0	116.6	117.0(5)	116.6(5)
$\angle C_4C_1H_8$	ζ	114.8	113.1	114.8(5)	113.1(5)
$\angle C_1C_4H_9$	ρ_1	111.5	110.2	111.5(5)	110.2(5)
$\angle C_1C_4H_{10}$	ρ_2	110.0	110.2	110.0(5)	110.2(5)
$\angle N_5C_4H_9$	π_1	108.0	108.6	108.0(5)	108.6(5)
$\angle N_5C_4H_{10}$	π_2	108.2	108.6	108.2(5)	108.6(5)
$\angle H_9C_4H_{10}$	χ	107.8	108.4	107.8(5)	108.4(5)
$\tau N_5C_4C_1C_2$	τ_1	78.7	−35.6	80.2(10)	−35.5(5)
$\tau N_5C_4C_1C_3$	τ_1	148.5	35.6	149.6(10)	35.5(5)
$\tau N_5C_4C_1H_8$	τ_1	−65.6	180	−64.5(10)	180
$\tau S_7C_6N_5C_4$	τ_2	178.5	180	177.6(5)	180
$\tau C_6N_5C_4C_1$	τ_3	−18.4	180	−18.4(5)	180
$\tau H_9C_4C_1N_5$		120.6	120.2	120.6(5)	120.2(5)
$\tau H_{10}C_4C_1N_5$		−119.8	−120.2	−119.8(5)	−120.2(5)
A		5207.9	7071.7	5226.9	7059.2
B		1087.8	889.2	1084.5	891.4
C		939.7	847.3	939.2	849.3
k		−0.9306	−0.9865	−0.9322	−0.9864
$\lvert\mu_a\rvert$		3.569	3.003		
$\lvert\mu_b\rvert$		0.378	1.630		
$\lvert\mu_c\rvert$		0.065	−		
$\lvert\mu_t\rvert$		3.589	3.417		

corresponding *gauche*−*cis* bands at 1322 and 1386 cm^{-1}, and both are symmetrical and well-defined, which makes them ideal for ΔH determinations. However, the two *gauche*−*cis* bands could not be used as they appeared to have underlying bands.

Three *gauche*−*cis* bands, all of them well-resolved and well-separated, were also used for the conformational stability determination. The *gauche*−*cis* bands are assigned to (ring)-CH_2 rock (ν_{25}) at 833 cm^{-1}, ring deformation (ν_{23}) at 930 cm^{-1}, and CH_2 rock (ν_{22}) at 991 cm^{-1}. The intensities of the infrared bands were measured as a function of temperature, and their ratios were determined. By application of the van't Hoff equation $-\ln K = \Delta H/(RT) - \Delta S/R$, ΔH was determined from a plot of $-\ln K$ versus $1/T$, where $\Delta H/R$ is the slope of the line and K is substituted with the appropriate intensity ratios, i.e., $I_{gauche-cis}/I_{cis-trans}$. It was assumed that ΔH is not a function of temperature in the temperature range studied.

By combining the three *gauche*−*cis* and the two *cis*−*trans* conformer bands, six pairs of bands (Figure 6) were utilized for the determination of the enthalpy difference. The resulting values with statistical uncertainties are listed in Table 5. The average of these six values by utilizing all the data as a single set is 228 ± 6 cm^{-1}, where the error limit is derived from the statistical standard deviation of the measured intensity data. These error limits do not take into account small associations with the liquid xenon or the interference of overtones and combination bands in near coincidence with the measured fundamentals. To minimize the possibility for interference from overtones and combination bands (only few possibilities below 400 cm^{-1}) in the determination of the enthalpy difference, we recorded the temperature-dependent far-infrared spectra (100−400 cm^{-1}) of cyclopropylmethyl isothiocyanate in liquid krypton. However, no conformer pair was found from which an enthalpy difference could be determined. A more reasonable uncertainty is therefore estimated to be 10%, which corresponds to a final value of 228 ± 23 cm^{-1} (2.73 ± 0.27 kJ·mol^{-1}) reported for the enthalpy difference between the two conformers.

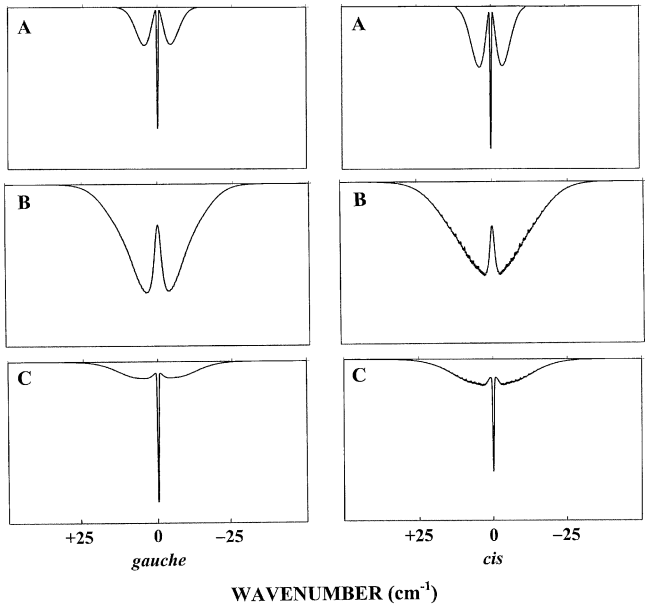

Figure 5. Predicted pure *A*-, *B*- and *C*-type gas-phase infrared band contours for the *gauche*−*cis* and *cis*−*trans* conformers of cyclopropylmethyl isothiocyanate.

Thus, given statistical weights of 2:1, respectively, for the *gauche*−*cis* and *cis*−*trans* forms, the abundance of the less stable *cis*−*trans* conformer present at ambient temperature is 14 ± 2%.

A comparison with the theoretical results shows that the MP2 calculations with diffuse functions provide much closer predictions to the experimentally determined conformational enthalpy difference than those without diffuse functions. The average of the predicted energy difference from MP2 calculations with diffuse functions is 226 cm^{-1}, which is only 2 cm^{-1} from the experimental value. However, the average of the predicted energy difference from MP2 calculations without diffuse functions is only 60 cm^{-1}, about 1/4 of the experimental value. The inclusion of diffuse functions has a smaller effect on density functional theory calculations; for the B3LYP method, the average predicted energy difference with diffuse functions is 254 cm^{-1} and that without diffuse functions is 187 cm^{-1}; the former is only slightly (3 cm^{-1}) larger than the estimated upper limit of experimental error, whereas the latter is 18 cm^{-1} lower than the lower experimental limit. An average of all B3LYP-predicted values studied yields an energy difference of 220 cm^{-1}, which agrees very well with the experimental value. Similarly, strong dependence on the inclusion of diffuse functions for predicting the correct conformational energy differences was found for some other monosubstituted methylcyclopropane compounds, e.g., fluoromethyl cyclopropane[1] and aminomethyl cyclopropane.[17] Thus, it seems that diffuse functions are necessary for more accurate predictions on conformational stabilities of certain monosubstituted methylcyclopropane molecules.

Structural Parameters

To the best of our knowledge, no structural study has been published for cyclopropylmethyl isothiocyanate. However, microwave investigations have been carried out for isothiocyanic acid[18] (HNCS) and the r_s structural parameters determined. These parameters have been compared[19] to those predicted from ab initio MP2(full)/6-311+G(d,p) calculations along with adjustments by utilizing the microwave reported rotational constants, which required the N═C distance be reduced by 0.008 Å from the predicted value, the C═S distance slightly elongated by 0.001 Å, and the NCS angle increased by 0.2°. From this information, the structural parameters for the NCS substituent can be estimated. Similarly the two most stable *gauche*−*gauche-1 and gauche*−*trans* conformations of aminomethylcyclopropane, which share the same *c*-$C_3H_5C(H_2)$ orientation with the title compound, were obtained[17] by the adjustments of the predicted parameters from the MP2(full)/6-311+G(d,p) calculation with the reported[20] microwave rotational constants. Thus, we have attempted to estimate the r_0 structural parameters of cyclopropylmethyl isothiocyanate by systematically adjusting the predicted ab initio parameters in the same

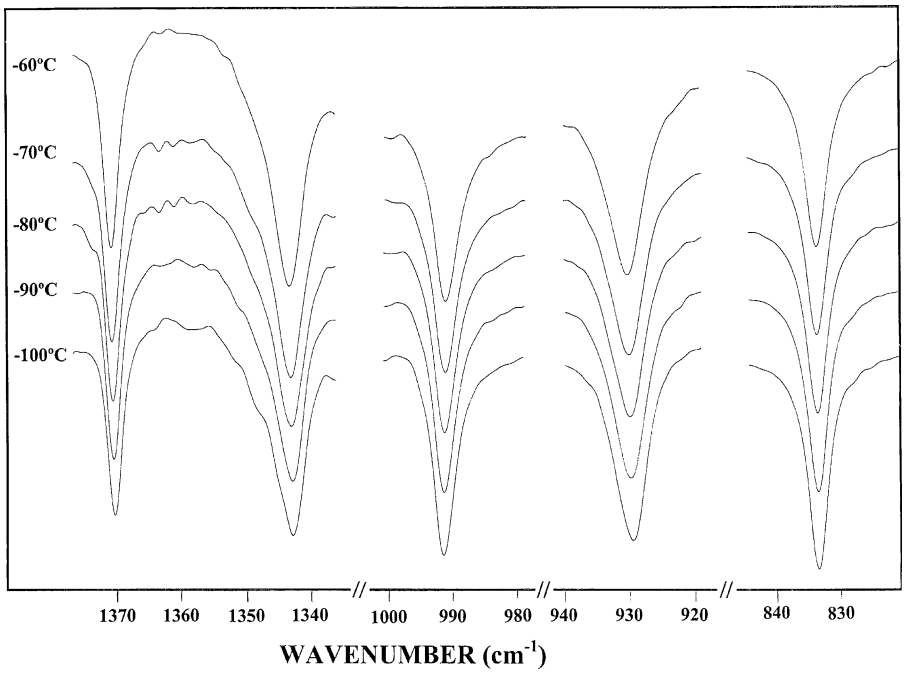

Figure 6. Temperature (−55 to −100 °C) dependence of the 1343, 1370 cm^{-1} *cis*−*trans* bands and the 833, 930, 991 cm^{-1} *gauche*−*cis* bands in the mid-infrared spectra of cyclopropylmethyl isothiocyanate dissolved in liquid xenon.

TABLE 5: Temperature-Dependent Intensity Ratios for the *gauche*−*cis* and *cis*−*trans* Conformers of Cyclopropylmethyl Isothiocyanate Dissolved in Liquid Xenon

T (°C)	1000/T (K^{-1})	I_{833gc}/I_{1343ct}	I_{833gc}/I_{1370ct}	I_{930gc}/I_{1343ct}	I_{930gc}/I_{1370ct}	I_{991gc}/I_{1343ct}	I_{991gc}/I_{1370ct}
−55.0	4.5840	5.26856	7.01736	2.38626	3.17833	22.10506	29.44240
−60.0	4.6915	5.54704	7.47562	2.44572	3.29604	23.09919	31.13024
−65.0	4.8042	5.93113	7.51004	2.59402	3.28457	24.93430	31.57200
−70.0	4.9225	6.15385	7.92033	2.70278	3.47862	25.77151	33.16930
−75.0	5.0467	6.58068	8.20948	2.76782	3.45290	27.30769	34.06671
−80.0	5.1773	6.85009	8.52420	2.88520	3.59032	28.51518	35.48406
−85.0	5.3149	7.24735	9.41839	2.94033	3.82114	29.46583	38.29268
−90.0	5.4600	7.57813	9.68185	3.06982	3.92202	30.79590	39.34498
−95.0	5.6132	8.30343	10.40462	3.28601	4.11753	33.35725	41.79833
−100.0	5.7753	8.48640	10.48827	3.36583	4.15980	33.96614	41.97844
ΔH (cm^{-1})	individual pair	282 ± 9	248 ± 12	201 ± 8	166 ± 9	252 ± 11	217 ± 10
ΔH (cm^{-1})	statistical[a] average	228 ± 6					

[a] All data as single set.

fashion as required for HNCS and the *c*-$C_3H_5C(H_2)$ moiety in aminomethylcyclopropane such that the resulting predicted r_0 parameters should closely reproduce the microwave rotational constants.

In addition, we[21] have recently shown for more than fifty carbon−hydrogen distances that MP2(full)/6-311+G(d,p) predicted r_e distances match the ground-state r_0 distances to within 0.002 Å of the experimentally determined values from "isolated" CH stretching frequencies.[22] Considering this level of accuracy in the CH predictions as well as the small mass of the hydrogen atom, the effect on the rotational constants from the very small errors in MP2(full)/6-311+G(d,p) predicted CH bond distances are orders of magnitude smaller than the similar errors from the skeletal structure. Thus, it is possible to further reduce the number of independent parameters by fixing CH parameters as MP2(full)/6-311+G(d,p) optimized values. It has also been shown[23] that MP2(full)/6-311+G(d,p) calculations predict the C−C distances very well for cyclopropane and methylcyclopropane. Thus, it appears that a reasonable level of calculation upon which the structural adjustments can be made with confidence for these ring compounds is MP2(full)/6-311+G(d,p).

By transferring the adjustments of the NCS moiety from HNCS[19] and the adjustments of the *c*-$C_3H_5C(H_2)$ moiety from aminomethylcyclopropane,[17] the estimated r_0 structure for cyclopropylmethyl isothiocyanate is proposed for both the *gauche*−*cis* and the *cis*−*trans* forms (Table 4). Ab initio predictions of the C_1-C_4, C−N, N=C, and C=S distances are adjusted by +0.0024, −0.0024, −0.008, and +0.001 Å, respectively. The C−C distances in the ring are elongated by 0.002 to 0.004 Å. The ab initio ∠CCN skeletal angle is increased by 0.2°, and the $\angle XC_2C_5$ angle (X is a dummy equidistant to the three apexes of the ring) decreased by 0.25°. The estimated uncertainties of the proposed structural parameters are ±0.002 Å for C−H distances, ±0.005 Å for all other bond lengths, ±0.5° for all bond angles, and ±1.0° all dihedral angles with the exception of the torsional dihedral angles along the C_5-N_6 bond in the *gauche*−*cis* form, which are closely associated with the low-barrier large-amplitude torsion and are, thus, predicted and adjusted with the largest uncertainty (±2.0°). Thus, the accuracy of the adjusted A, B, and C rotational constants of the *gauche*−*cis* form are strongly dependent on the quality of the $\tau(C_2C_5N_6C_8)$ dihedral prediction. The rotational constants as functions of $\tau(C_2C_5N_6C_8)$ are plotted in Figure 7. It is expected that this information on the estimated structure will facilitate possible future microwave investigation of cyclopropylmethyl isothiocyanate.

Discussion

Two scaling factors of 0.88 and 0.90 have been used with the MP2(full)/6-31G(d) calculations to obtain the predicted vibrational frequencies, which are in good agreement with the observed values. The average error in the frequency predictions for the normal modes of the *gauche*−*cis* conformers is 12 cm^{-1}, which represents an error of only 0.9% with the largest sources from the ν_{23} ring deformation, ν_6 and ν_7 methylene CH_2 stretches and ν_{21} (ring)CH_2 wag. Thus, multiple scaling factors are not necessary for predicting the frequencies of normal modes, particularly, for distinguishing those for the two different conformers.

Because the structural parameters for the two conformers differ very little, most of the corresponding force constants are nearly the same from scaled MP2(full)/6-31G(d) results (Table 1S, Supporting Information). The largest force constant difference between the two forms is the ring torsion where the *cis*−*trans* force constant is twice that for the *gauche*−*cis* form. In addition, $\angle C_1C_4N_5$, $\angle C_3C_1C_4$, and $\angle C_2C_1C_4$ bends also involve large force constant differences with the *cis*−*trans* values larger by 23, 15, and 10%, respectively. On the other hand, the $\angle C_4N_5C_6$ bend as well as the C=N torsion force constants of the *gauche*−*cis* conformer are larger than those of the *cis*−*trans* by 20 and 17%, respectively. These changes reflect significant differences in skeletal angles and dihedrals between conformations. The largest conformational difference in CH bending force constants is the 7% difference for $\angle C_1C_4H_8$ with the *cis*−*trans* conformer having the larger value. For all other force constants, the differences are less than 4% between the *gauche*−*cis* and *cis*−*trans* conformers with most of them involving differences less than 1%.

Cyclopropylmethyl isothiocyanate has two major resonance structures, *c*−$C_3H_5CH_2-N=C=S$ and *c*−$C_3H_5CH_2-N^+\equiv C-S^-$, with the first resonance structure assuming an sp^2 hybridization on the nitrogen atom with a bent C−N=C angle, and the second one with sp hybridization on the nitrogen atom assuming a charged linear $C-N^+\equiv C-S^-$ structure. The ground-state structures calculated with MP2 and B3LYP methods for the *gauche*−*cis* and the *cis*−*trans* forms are between the two resonance structures. However, low-level restricted Hartree−Fock calculations predict an almost linear CNCS structure for the molecular ground states, which is due to the method's inadequate treatment of electron correlation, especially along the multiply bonded NCS moiety. Of the structural parameters listed in Table 4, it is interesting to note that the CNC angles are calculated to be 140.1 and 144.0° for the *gauche*−*cis* and *cis*−*trans* forms, respectively, whereas this angle is

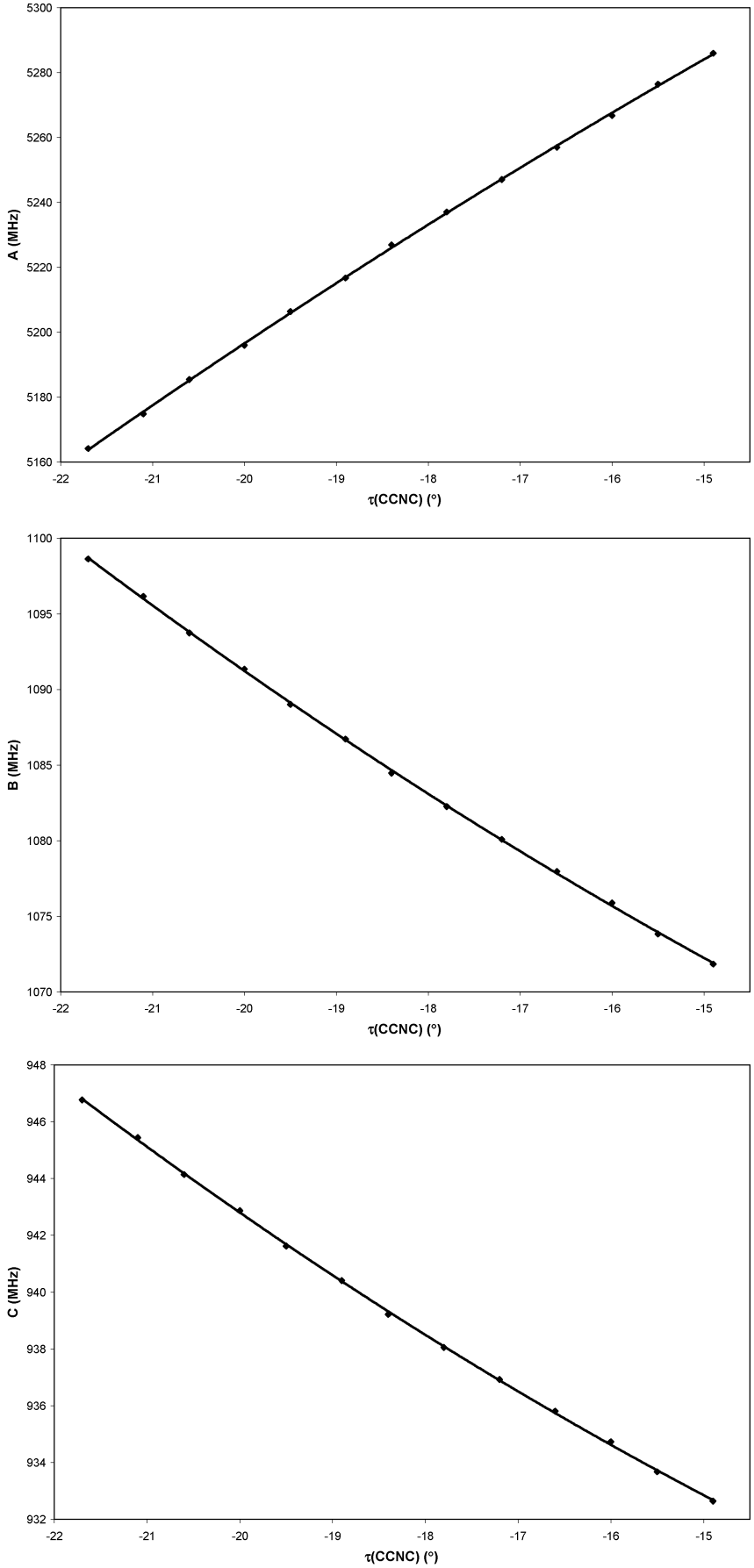

Figure 7. Adjusted *A*, *B*, and *C* rotational constants of the *gauche*−*cis* form as functions of the $\tau(C_2C_5N_6C_8)$ dihedral angle.

expected to be ∼120° for the first resonance structure and 180° for the second. Additionally, the NC distances in the NCS moiety are between those of the double and triple bonds. The NC distances are predicted to be 1.210 and 1.208 Å and adjusted

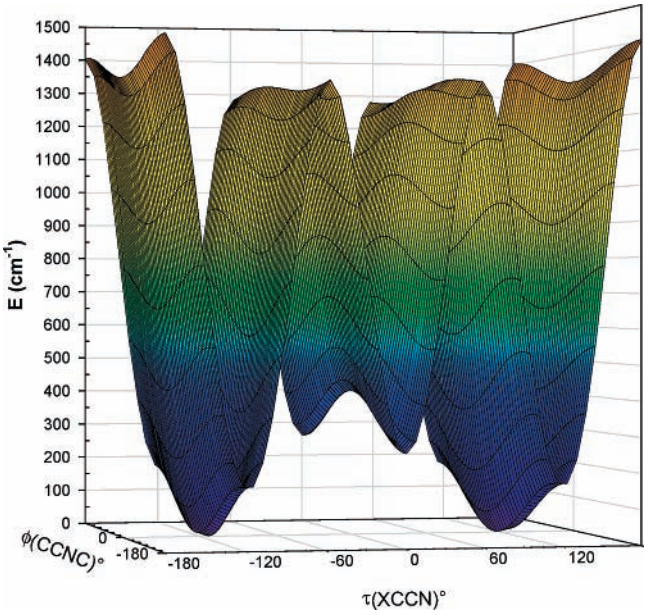

Figure 8. Theoretical potential surface governing τ(XCCN) and ϕ(CCNC) torsions in cyclopropylmethyl isothiocyanate, calculated at MP2(full)/6-31G(d) level.

to 1.202 and 1.200 Å, respectively, for the *gauche*−*cis* and *cis*−*trans* forms, whereas a typical N═C distance is 1.273 Å (methyleneimine[24]) and that of a typical N≡C distance is 1.156 Å (hydrogen cyanide[25]). The CS distances are predicted to be 1.577 and 1.576 Å and adjusted to 1.578 and 1.577 Å, respectively, for the *gauche*−*cis* and *cis*−*trans* forms; the bond distances are between the typical C−S distance of 1.814 Å (methanethiol[26]) and the typical (═)C═S distance of 1.554 Å (thiocarbonyl thioketene[27]).

The conformational interchange of cyclopropylmethyl isothiocyanate involves the τ(XCCN) dihedral angle (where X is a dummy atom at the center of the three-membered ring equidistant to the three apexes) and the ϕ(CCNC) dihedral angle. In the context of our conformational energetics study, the potential energy of the molecule is considered to be a function of these two dihedral angles, τ and ϕ. The resulting three-dimensional potential surface is shown in Figure 8. The most stable *gauche*−*cis* (τ =117.7°, ϕ =0.7°) conformer corresponds to the global minimum whereas the less stable *cis*−*trans* conformer corresponds to a local minimum. The *cis*−*cis* and *gauche*−*trans* forms correspond to first-order saddle points. The global maximum corresponds to the *trans*−*trans* orientation. The cross-section along the τ(XCCN) dihedral is a *gauche*−*cis*−*gauche* type 3-fold potential, whereas the one along the ϕ(CCNC) dihedral is a *cis*−*trans* type monotonic 1-fold potential. In addition, the function describing the potential energy surface, E(τ,ϕ), must conform to the following symmetry restrictions $E(\tau,\phi) = E(-\tau,-\phi) \neq E(-\tau,\phi) = E(\tau,-\phi)$. Thus, by applying the common approach of fitting Fourier series to represent two-dimensional potential curves, the three-dimensional surface should take on the general form of:

$$E(\tau,\phi) = 1/2\sum_i [V_{i0} + 1/2\sum_j V_{ij}(1 - \cos j\phi)](1 - \cos i\,\tau) + 1/4\sum_i\sum_j V'_{ij} \sin j\,\phi \sin i\,\tau + 1/2\sum_j V_{0j}(1 - \cos j\,\phi) + V_{00}$$

where the first term is the Fourier cosine series of τ, describing the potential curve along the τ(XCCN) dihedral. The Fourier cosine coefficients, which are constants in the two-dimensional curve, are now a function of the ϕ(CCNC) dihedral, and they are fitted by another Fourier cosine series of ϕ. Similarly, the second term is the Fourier sine series of the τ(XCCN) dihedral where the sine coefficients are now fitted by another Fourier sine series of the ϕ(CCNC) dihedral. The third term describes the symmetric potential curve as a function of the ϕ(CCNC) dihedral, along the τ(XCCN) = 0 (ring cis to NCS) cross-section. The last term, V_{00}, is a constant equal to the energy difference between the *cis*−*cis* ($\tau = \phi = 0$, first-order saddle point) structure and the most stable *gauche*−*cis* conformations.

TABLE 6: Calculated (B3LYP/6-31G(d)) Fourier Coefficients of the Potential Surface for the Two-Dimensional Conformational Interchange of Cyclopropylmethyl Isothiocyanate

Fourier Cosine Series Coefficients (cm^{-1})			
V_{10}	−282.97	V_{11}	274.69
V_{20}	−342.93	V_{21}	188.35
V_{30}	1146.17	V_{31}	−26.88
V_{40}	35.95	V_{41}	−28.27
V_{50}	37.70	V_{51}	−7.44
V_{60}	−54.32	V_{61}	7.83
Fourier Sine Series Coefficients (cm^{-1})			
V'_{11}	−43.13		
V'_{21}	−26.86		
V'_{31}	81.03		
V'_{41}	27.62		
Energy Correction Coefficients (cm^{-1})			
V_{01}	−153.82		
V_{00}	416.78		

Our analysis shows that for the 3-fold potential along the τ(XCCN) dihedral, only the first six Fourier cosine terms and the first four Fourier sine terms are significant, whereas for the 1-fold potential along the ϕ(CCNC) dihedral, only the first cosine term is significant. Thus, the potential surface, $E(\tau,\phi)$, can be reduced to the following form:

$$E(\tau,\phi) = 1/2\sum_{i=1}^{6}[V_{i0} + 1/2V_{i1}(1 - \cos\phi)](1 - \cos i\,\tau) + 1/4\sum_{i=1}^{4} V'_{i1} \sin\phi \sin i\,\tau + 1/2V_{01}(1 - \cos\phi) + V_{00}$$

The cosine terms V_{10}−V_{60} are analogous to the V_1−V_6 terms of the two-dimensional potential of the type $E(\tau) = 1/2\ \sum_{i=1}^{6} V_i(1 - \cos i\,\tau) + 1/2\ \sum_{i=1}^{4} V'_i \sin i\,\tau + V_0$, except for the additional ϕ fluctuations in the form of $1/2V_{i1}(1 - \cos\phi)$. Similarly, the sine term products of $1/2V'_{11}\cdot\sin\phi$−$1/2V'_{41}\cdot\sin\phi$ are analogous to the V'_1−V'_4 terms, except for the ϕ dependence. The resulting least-squares-fitted potential coefficients for this two-dimensional conformational interchange of cyclopropylmethyl isothiocyanate are listed in Table 6.

To account for the *cis* stability of ethynylmethyl cyclopropane, Dakkouri and Typke[28] recently proposed that the attractive interaction between the acidic hydrogen of the ethynyl group and the surface orbitals of the ring is a major factor. Such argument cannot be applied to explain the relative stability of the *cis* conformation (only 54 ± 4 cm^{-1} less stable than the *gauche* form,[4] compared with ∼300 cm^{-1} for the halogens) in cyanomethyl cyclopropane, where the terminal nitrogen atom is negatively charged. In addition, due to the extremely large distance between the acetylene hydrogen and the center of the three-membered ring (4.447 Å, calculated at MP2(full)/6-311+G(d,p) level), the "hydrogen-bonding" proposed is too weak to be the major factor contributing to the *cis* stability.

TABLE 7: Comparisons of Factors Contributing to the Relative Conformational Stability of a Series of Monosubstituted Methylcyclopropane Molecules

substituent	ref	$\Delta H_{cis} - \Delta H_{gauche}$ (cm^{-1})	electronegativity of substituents	MP2/6-311+G(d,p) r_e[(H_2)C-terminal atom)] (Å)	van der Waals radii[e] of terminal atoms (Å)	natural charge on substituent (*e*) g, *gauche*; c, *cis*
−C≡C*H	[5]	−147 ± 14	3.074[a]	3.748 g 3.746 c	H 1.20	C −0.00691 g, −0.00970 c C* −0.24683 g, −0.24920 c H +0.22307 g, +0.22500 c total −0.03067 g, −0.03390c
−C≡N	[4]	54 ± 4	3.208[a]	2.640 g 2.638 c	N 1.55	C +0.32966 g, +0.32962 c N −0.38443 g, −0.38690 c total −0.05477 g, −0.05728 c
−NCS	this study	228 ± 23	3.505[a]	4.033[c]g 4.065[c]c	S 1.80	N −0.57906 g, −0.59146 c C +0.38509 g, +0.39677 c S −0.09659 g, −0.09574 c total −0.29056 g, −0.29043 c
−F	[1]	262 ± 26	3.98[b]	1.399 g 1.395 c	F 1.47	F −0.44666 g, −0.44602 c
−Cl	[2]	274 ± 21	3.16[b]	1.791 g 1.783 c	Cl 1.75	Cl −0.10686 g, −0.10083 c
−Br	[2]	383 ± 29	2.96[b]	1.954 g 1.945 c	Br 1.85	Br −0.05054 g, −0.04022 c
$-CH_3$	[3]	∼385	2.472[a]	2.173[d]g 2.325[d]g	H 1.20	C −0.48763 g, −0.49629 c H +0.17003, +0.16580, +0.16919 g; +0.17505, +0.16691, +0.16691 c total +0.01739 g, +0.01258c

[a] Calculated group electronegativities from ref 29. [b] Pauling scale electronegativity. [c] Nonlinear CNCS connectivity. [d] Nonlinear CCH connectivity, average of three nonbonding CH distances. [e] Reference 30.

Dakkouri and Typke[28] also proposed that the electronegativity of the substitutent is the dominating factor determining conformational stability, i.e., the amount of *cis* conformer present at ambient temperature increases with increasing electronegativity of the substituent. Although the argument agrees with the experimental results for halomethyl cyclopropanes, clear discrepancies from such an argument arise from a comparison of the experimental conformational enthalpy differences and previously reported "group electronegativities"[29,30] listed in Table 7. For example, the electronegativity of fluorine (3.98, Pauling scale) is significantly larger than those of cyano (3.208) and ethynyl (3.074) groups, and the sizes of cyano and ethynyl groups are significantly larger than the fluorine atom; thus, it follows from the argument of Dakkouri and Typke[28] that fluoromethyl cyclopropane should have significantly larger *cis* population than the two triply bonded molecules. However, contrary to such prediction, experimental results showed that the *gauche* conformer of fluoromethyl cyclopropane[1] is more stable than the c*is* form by 262 ± 26 cm^{-1}, whereas the *cis* form is more stable in ethynylmethyl cyclopropane[5] by 147 ± 14 cm^{-1}, and the *gauche* form is more stable in cyanomethyl cyclopropane[4] by only 54 ± 4 cm^{-1}. A number of other discrepancies between Dakkouri and Typke's[28] proposed stability and experimental values regarding several substituents, e.g., between −F and −NCS, −NCS and −C≡CH, −NCS and −C≡N, −C≡CH and −C≡N, and −Cl and −C≡CH, can be found in Table 7. Therefore, electronegativity alone clearly cannot account for the observed conformational stabilities.

One factor contributing to almost all conformational stability considerations is the steric factor. The sizes of the monatomic halogen substituents can be evaluated by the (H_2)C−X distances plus van der Waals radius of the corresponding halogen atom (Table 7). The sizes of polyatomic substituents, including −C≡CH and −C≡N with linear structure as well as −NCS and $-CH_3$ with nonlinear structures, can be estimated by the distances between the methylene carbon and the terminal atom of the substituent plus the van der Waals radius of the terminal atom (Table 7). The steric factor argument seems to agree with the halogen series results, because with the increase of size from fluorine to bromine, the *gauche* conformer is gaining increased stability over the *cis* form. However, the steric argument cannot be used to explain the smaller conformational enthalpy differences associated with bulkier −C≡CH, −C≡N, and −NCS substituents, compared with the halogens.

Another important factor to be considered is the electrostatic interaction between the ring and the substituent in the *cis* conformer versus the methylene hydrogen in the *gauche* form. The Walsh-type orbitals of the three-membered ring give rise to the relatively large negative charge on the ring. The sign and the magnitude of the charge on the substituent determine the direction and strength of the electrostatic interaction between itself and the ring, i.e., the conformational stability. In going from the *cis* to the *gauche* form, the ring-to-(C−X) orientation goes from *cis* to *gauche*, whereas the ring-to-(C−H) orientation goes from *gauche* to *cis*. A more negatively charged substituent results in a greater preference for the *gauche* conformer because it introduces less electrostatic repulsion with the ring as well as greater electrostatic attraction between the hydrogen atom and the ring. A positively charged substituent, on the other hand, gives preference to the *cis* conformer.

In the treatment of polyatomic groups, atomic charges of each individual atom should be considered; however, the first connecting atom on the substituent has a more pronounced effect than the remaining atoms of the substituent, due to its closer distance to the three-membered ring. In cyanomethyl cyclopropane, the carbon atom on the cyano group takes on a relatively large positive charge (Table 7) which stabilizes the *cis* conformer. Although the total group charge remains negative, the positively charged carbon atom in the *cis* conformer is almost level with the top of the ring, and the short distance makes the electrostatic attraction stronger than the repulsion between the more distant negatively charged nitrogen and the ring. In the case of ethynylmethyl cyclopropane, the negative charge on the inside carbon of the substituent is one or two magnitudes smaller than the halogen series, making the electrostatic repulsion between the inside carbon and the ring at least an order of magnitude smaller. Meanwhile, the total ethynyl group charge is the least negative of the entire series; thus, the significantly

smaller electrostatic repulsion between the ethynyl group and the ring in the *cis* position contributes to the *cis* stability of ethynylmethyl cyclopropane.

For the halogen series from fluorine to bromine, the natural charges on the halogen substituents become less negative, which in turn would be expected to give rise to increased stability of the *cis* conformer. However, with the electronegativity and steric factor being more dominant, the contribution from electrostatic interaction is not large enough to change the order of conformational stability. Nevertheless, electrostatic effects can be used to explain the very close enthalpy differences for fluoro- and chloromethylcyclopropane, in which the significantly larger negative charge on the fluorine almost offsets the decrease of steric hindrance in going from chlorine to fluorine.

Because cyclopropylmethyl isothiocyanate has the largest group size of the series plus the most negative charge on the neighboring atom, it is expected to have the largest conformational enthalpy difference (larger than 385 cm^{-1}). On the other hand, the −NCS group's second largest electronegativity (next only to fluorine) of the series should lead to a relatively small conformational enthalpy difference (comparable to those of the fluoride's 262 ± 26 cm^{-1} and the chloride's 274 ± 21 cm^{-1}). Within the error limits, the three values are the same. Nevertheless, the conflicting influences from different factors make the explanation of the conformational stability rather difficult since the weight of each factor cannot be universally set.

As a result, a combination of electrostatic, electronegativity, steric, and orbital delocalization factors should be considered in the explanation of the relative conformational stabilities of monosubstituted methylcyclopropanes. However, a reliable prediction of the conformational stabilities based on the quantitative analysis of the contribution of these factors is still to be achieved.

Acknowledgment. We thank Prof. James M. Benevides and Prof. George J. Thomas of the School of Biological Sciences, University of Missouri—Kansas City, for collecting the Raman spectrum. We also thank Ms. Lakshmi Chakka, who performed some of the initial ab initio calculations on these molecules. We acknowledge the University of Missouri—Kansas City for a faculty research grant (J.R.D.) and faculty development leave (C.J.W.) for support of this research.

Supporting Information Available: Table 1S, scaled diagonal force constants from MP2(full)/6-31G(d) ab initio calculations for cyclopropylmethyl isothiocyanate; Table 2S, symmetry coordinates of cyclopropylmethyl isothiocyanate. This material is available free of charge via the Internet at http://pubs.acs.org.

References and Notes

(1) Durig, J. R.; Yu, Z.; Zheng, C.; Guirgis, G. A. *J. Phys. Chem. A* **2004**, *108*, 5353.

(2) Durig, J. R.; Shen, S.; Zhu, X.; Wurrey, C. J. *J. Mol. Struct.* **1999**, *485*, 501.

(3) Wurrey, C. J.; Shen, S.; Gounev, T. K.; Durig, J. R. *J. Mol. Struct.* **1997**, *405*, 207.

(4) Wurrey, C. J.; Shen, S.; Zhu, X.; Zhen, H.; Durig, J. R. *J. Mol. Struct.* **1998**, *449*, 203.

(5) Guirgis, G. A.; Wurrey, C. J.; Yu, Z.; Zhu, X.; Durig, J. R. *J. Phys. Chem. A* **1999**, *103*, 1509.

(6) Frisch, M. J.; Trucks, G. W.; Schlegel, H. B.; Scuseria, G. E.; Robb, M. A.; Cheeseman, J. R.; Montgomery, J. A., Jr.; Vreven, T.; Kudin, K. N.; Burant, J. C.; Millam, J. M.; Iyengar, S. S.; Tomasi, J.; Barone, V.; Mennucci, B.; Cossi, M.; Scalmani, G.; Rega, N.; Petersson, G. A.; Nakatsuji, H.; Hada, M.; Ehara, M.; Toyota, K.; Fukuda, R.; Hasegawa, J.; Ishida, M.; Nakajima, T.; Honda, Y.; Kitao, O.; Nakai, H.; Klene, M.; Li, X.; Knox, J. E.; Hratchian, H. P.; Cross, J. B.; Bakken, V.; Adamo, C.; Jaramillo, J.; Gomperts, R.; Stratmann, R. E.; Yazyev, O.; Austin, A. J.; Cammi, R.; Pomelli, C.; Ochterski, J. W.; Ayala, P. Y.; Morokuma, K.; Voth, G. A.; Salvador, P.; Dannenberg, J. J.; Zakrzewski, V. G.; Dapprich, S.; Daniels, A. D.; Strain, M. C.; Farkas, O.; Malick, D. K.; Rabuck, A. D.; Raghavachari, K.; Foresman, J. B.; Ortiz, J. V.; Cui, Q.; Baboul, A. G.; Clifford, S.; Cioslowski, J.; Stefanov, B. B.; Liu, G.; Liashenko, A.; Piskorz, P.; Komaromi, I.; Martin, R. L.; Fox, D. J.; Keith, T.; Al-Laham, M. A.; Peng, C. Y.; Nanayakkara, A.; Challacombe, M.; Gill, P. M. W.; Johnson, B.; Chen, W.; Wong, M. W.; Gonzalez, C.; Pople, J. A. *Gaussian 03*, revision B.04; Gaussian, Inc.: Pittsburgh, PA, 2003.

(7) Pulay, P. *Mol. Phys.* **1969**, *179*, 197.

(8) Badawi, H. M. Department of Chemistry, King Fahd University of Petroleum and Minerals, Dhahran, Saudi Arabia. Personal communication, 2004.

(9) Gurigis, G. A.; Zhu, X.; Yu, Z.; Durig, J. R. *J. Phys. Chem. A* **2000**, *104*, 4383.

(10) Frisch, M. J.; Yamaguchi, Y.; Gaw, J. F.; Schaefer, H. F., III; Binkley, J. S. *J. Chem. Phys.* **1986**, *84*, 531.

(11) Amos, R. D. *Chem. Phys. Lett.* **1986**, *124*, 376.

(12) Polavarapu, P. L. *J. Phys. Chem.* **1990**, *94*, 8106.

(13) Chantry, G. W. In *The Raman Effect*, Vol. 1; Anderson, A., Ed.; Marcel Dekker Inc.: New York, 1971; Chapter 2.

(14) Herrebout, W. A.; van der Veken, B. J. *J. Phys. Chem.* **1996**, *100*, 9671.

(15) Herrebout, W. A.; van der Veken, B. J.; Wang, A.; Durig, J. R. *J. Phys. Chem.* **1995**, *99*, 578.

(16) van der Veken, B. J.; DeMunck, F. R. *J. Chem. Phys.* **1992**, *97*, 3060.

(17) Durig, J. R.; Zheng, C.; Warren, R. D.; Groner, P.; Wurrey, C. J.; Gounev, T. K.; Herrebout, W. A.; van der Veken, B. J. *J. Phys. Chem. A* **2003**, *107*, 7713.

(18) Yamada, K.; Winewisser, M.; Winewisser, G.; L. Szalanski, B. M.; Gerry, C. L. *J. Mol. Spectrosc.* **1980**, *79*, 295.

(19) Durig, J. R.; Zheng, C.; Deeb, H. *J. Mol. Struct.* in press.

(20) Marstokk, K. M.; Møllendal, H. *Acta Chem. Scand. A* **1984**, *38*, 387.

(21) Durig, J. R.; Ng, K. W.; Zheng, C.; Shen, S. *Struct. Chem.* **2004**, *5*, 149.

(22) McKean, D. C.; Torto, I. *J. Mol. Struct.* **1982**, *81*, 51.

(23) Durig, J. R. in *Advances In Molecular Structure Research*, Vol. 6; Hargittai, M., Hargittai, I., Ed.; JAI Press Inc.: Stanford, CT, 2000.

(24) Pearson, R., Jr.; Lovas, F. J. *J. Chem. Phys.* **1977**, *66*, 4149.

(25) Pearson, E. F.; Creswell, R. A.; Winnewisser, M.; Winnewisser, G. *Z. Naturforsch. A* **1976**, *31*, 1394.

(26) Kojima, T. *J. Phys. Soc. Jpn.* **1960**, *15*, 1284.

(27) Georgiou, K.; Kroto, H. W.; Landsberg, B. M. *J. Mol. Spectrosc.* **1979**, *77*, 365.

(28) Dakkouri, M.; Typke, V. *J. Mol. Struct.* **2000**, *550*−*551*, 349.

(29) Inamoto, N.; Masuda, S. *Chem. Lett.* **1982**, 1003.

(30) Bondi, A. *J. Phys. Chem.* **1964**, *68*, 441.